Results in Optics 5 (2021) 100186

Contents lists available at ScienceDirect

Results in Optics

journal homepage: www.sciencedirect.com/journal/results-in-optics

# Optical design of the laser launch telescope via physical optics theorem for laser guide star facility

Yan Mo [a], Zhengbo Zhu [b,*], Zichao Fan [a], Donglin Ma [a,b,*]

[a] MOE Key Laboratory of Fundamental Physical Quantities Measurement & Hubei Key Laboratory of Gravitation and Quantum Physics, PGMF and School of Physics, Huazhong University of Science and Technology, Wuhan 430074, China
[b] School of Optical and Electronic Information and Wuhan National Laboratory for Optoelectronics, Huazhong University of Science and Technology, Wuhan 430074, China

ARTICLE INFO

*Keywords:*
The laser guide star facility
Laser lunch telescope
Optical design
Physical optics propagation

ABSTRACT

The Laser Guide Star Facility (LGSF), as the most important part of the adaptive optics system of the large ground-based telescope, is aimed to generate multiple laser guide stars at the sodium layer. Laser Launch Telescope is employed to implement this requirement by projecting the Gauss beam to the sodium layer with a small beam size in LGSF system. As the diffraction and interference effects of laser's long-distance transmission, the conventional optical design based on the geometrical optics mechanism cannot achieve the expected laser propagation. In this paper, we propose a method to design optical system for laser launch telescope based on the physical optics theorem to generate an acceptable light spot at the sodium layer in the atmosphere. Besides, a tolerance analysis method based on physical optics propagation is also demonstrated to be necessitated to optimize the system's instrumentation performance. The numerical results show that the optical design considering physical optics propagation is highly rewarding and even necessitated in many occasions, especially for laser beam propagation systems.

## 1. Introduction

The Laser Guide Star Facility (LGSF) is one of the most important parts of large ground-based telescopes to improve the capability in high-resolution imaging of faint stars. Specifically, it is used to generate artificial laser guide stars for adaptive optics (AO) systems to compensate for the perturbation caused by the atmosphere. The laser guide star technique was firstly put forward by Happer et al in 1982 (Happer et al., 1994) and then the experiment was implemented by Primmerman et al (Primmerman et al., 1991). In 2001, the laser guide star AO system with laser guide star was firstly installed on Keck I (Chin et al., 2012) and later on Keck II (Chin et al., 2016). With the continuous progress of astronomical optical technology, the laser guide star system projecting several asterisms was assembled on Gemini telescope in 2011 (d'Orgeville et al., 2012), which demonstrated the well performance and high reliability of the LGSF. From then on, the LGSF has been widely used by many other famous observatories including VLT (Hackenberg et al., 2014), Subaru (Minowa et al., 2012), and Thirty Meter Telescope (TMT) (Li et al., 2018), etc.

In order to project and expend the laser beam into sodium layer, a crucial component called Laser Launch Telescope (LLT) is employed in LGSF system. As for the optical requirements, the most important goal of LLT is to eliminate aberration as much as possible to generate an acceptable light spot among the sodium layer at a predefined altitude (120 km) and maintain a high ratio of encircled energy. Specifically, the RMS wavefront error (WFE) of the LLT design should be limited to a reasonable value. A high encircled energy ratio means a high energy utilization efficiency, which contributes to produce bright artificial laser guide stars.

As the long-distance of propagation of laser beam in free space, it is necessary to take the diffraction and interference effects into consideration in the optical design process of LLT. In other words, the optical design of LLT should be implemented in the physical optics theorem. However, it is almost impossible to conduct the optical design for LLT directly based on the physical optics theory simply relying on commercial optical design software such as ZEMAX. As a rule of thumb, an optimal design process is to design the initial optical structure with the assumption of geometrical optics approximation, and then optimize it

* Corresponding authors at: MOE Key Laboratory of Fundamental Physical Quantities Measurement & Hubei Key Laboratory of Gravitation and Quantum Physics, PGMF and School of Physics, Huazhong University of Science and Technology, Wuhan 430074, China (D. Ma).
*E-mail addresses:* zhuzb@hust.edu.cn (Z. Zhu), madonglin@hust.edu.cn (D. Ma).

https://doi.org/10.1016/j.rio.2021.100186
Received 22 August 2021; Received in revised form 16 October 2021; Accepted 1 November 2021
Available online 10 November 2021

based on the physical optics theorem.

In this paper, we propose a method to design optical system for LLT based on the physical optics theorem. In this method, we firstly analyze the physical propagation model of laser beam, then design the initial optical system of LLT based on the geometrical optics assumption. After that, the optical performance of the initial LLT is evaluated based on physical optics. The RMS wavefront error (WFE) and the encircled energy ratio are selected as the criteria for evaluation of optical performance. Next, the optical system is updated with the physical optics theorem to achieve the predefined optical requirements. Finally, we provide a tolerance analysis method based on Gauss beam propagation to predict the expected optical performance of LLT with instrumentation errors. For the finally obtained optical system, the encircled energy ratio within a diameter of 233 mm at 120 km exceeds 92.5% considering the tolerance allocation. And the largest RMS WFE is less than 0.016λ with the working temperature ranging from −5°C to 20 °C.

## 2. Design consideration

The LLT is a laser beam expander essentially. To avoid the extremely tight optical and mechanical tolerances, we choose the Galilei telescope as the initial structure of LLT. Additional advantages of this choice are the compact configuration and the avoidance of the internal focal point, which is beneficial to the mechanical fabrication. Only a single working wavelength (589 nm) is considered, and a Galilei telescope configuration with two singlets is employed. The optical layout of LLT is shown in Fig. 1.

For the general applications, the working temperature ranges from −5°C to 20 °C is considered. To reduce the difficulty of mechanical alignment, the distance between Lens 1 and Lens 2 is set as 850 mm in consideration of the general demands. Besides, the distance between Lens 1 and Lens 2 is expected to be adjustable within a range of ± 0.25 mm to compensate the performance degradation due to the manufacturing and assembly errors as well as the environmental disturbance. We choose the field of view (FOV) as 0.06° to match the general AO systems. As mentioned above, the main goal of LLT is to produce a small light spot at the sodium layer while maintaining high energy efficiency as much as possible, we select the RMS WFE and the enclosed energy ratio as the criteria for the evaluation of optical performance. Based on the science requirement of general AO systems, the radius of the light spot is usually limited to 233 mm at 120 km in altitude. The design specifications are expressly presented in Table 1.

## 3. Optical design

### 3.1. The geometrical optical design

The spherical aberration is the main error source that contributes the enclosed energy loss in the sodium layer. Based on Seidel sums (Gross et al., 2015), all of the primary aberrations coefficients of the given optical system can be numerically calculated. For the spherical aberration:

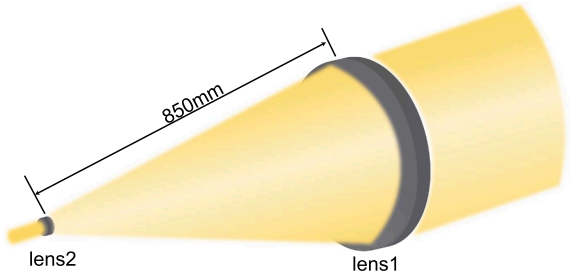


**Fig. 1.** Optical layout of LLT.

**Table 1**
Design requirements for LLT.

| Parameters | Value |
|---|---|
| Wavelength | 589 nm |
| Pupil position | Lens 1 |
| RMS WFE | 0.037λ |
| FOV | 0.06° |
| Working temperature | −5°C ~ 20 °C |
| Distance between Lens 1 and Lens 2 | 850 mm ± 0.25 mm |
| Radius of light spot | <233 mm |
| Encircled energy ratio | >90% |

$$S| = \frac{1}{4}\phi^3 y^3 \left(AX^2 - BXM + CM^2 + D\right) \tag{1}$$

$$W_{040} = \frac{1}{8}S| \tag{2}$$

where $\phi$ is the refractive power, $M$ represents the position or conjugate parameter, $X$ denotes the bending parameter and $A, B, C, D$ are constants related to the refractive index. The position or conjugate parameter $M$ is given by:

$$M = \frac{u' + u}{u' - u} = \frac{1 + m}{1 - m} \tag{3}$$

where $u$ and $u$' are the paraxial marginal ray angle before and after the lens respectively , $m$ stands for the magnification. The bending parameter $X$ determined by:

$$X = \frac{c_1 + c_2}{c_1 - c_2} \tag{4}$$

where $c_1$ and $c_2$ are curvatures of a lens. From Eq. (1), it is obvious that the spherical aberration $S_1$ depends on the square of the bending parameter $X$. Therefore a suitable choice of bending allocation for two lenses is necessitated to minimize spherical aberration. During the optimization progress, the location of the beam waist is constrained. The optimized optical parameters are listed in Table 2.

To evaluate the optical performance of the obtained optical system at different temperatures, the thermal analysis is implemented. Three different working temperatures including −5°C, 9 °C and 20 °C are considered. The distance between Lens 1 and Lens 2 is selected as the compensator. As illustrated in Fig. 2, the initial design shows a good optical performance under different working conditions and meets the requirement of RMS WFE over full FOV. However, the compensation distance reaches 0.5134 mm, which may not satisfy the mechanical constraint.

### 3.2. Physical optics performance

Note that, it is impossible to directly project the beam waist to the sodium layer by the above obtained optical system according to the relationship between beam waist location and waist size, which is given

**Table 2**
Optical parameter for LLT initial design.

| Element | Material | Curvature radius(mm) | Thickness (mm) | Conic | Semi-Diameter (mm) |
|---|---|---|---|---|---|
| Lens1-S1 | SILICA | 397.239 | 70.022 | −0.411 | 200 |
| Lens1-S2 | | 1641.119 | 920.000 | | 200 |
| Lens2-S1 | SILICA | −68.700 | 15.236 | −0.972 | 30 |
| Lens2-S2 | | 1120.145 | | | 30 |

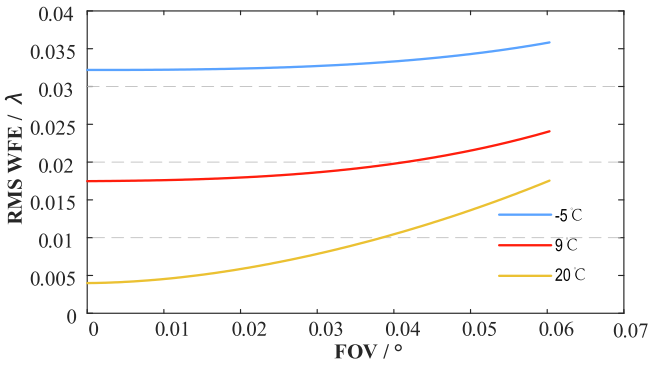


**Fig. 2.** RMS WFE Vs FOV for different temperature.

by

$$w = w_0^2\sqrt{(1+\frac{z^2}{f^2})} \tag{5}$$

where $w_0$ is the semi-diameter of the waist, $z$ represents the propagation distance, and $f$ demotes the rayleigh range. The output beam $1/e^2$ diameter is set as 240 mm to avoid beam clipping (Holzlöhner et al., 2008) referring to the existing designs (Bonaccini et al., 2003; d'Orgeville et al., 2002; Boyer et al., 2010). Based on the simulation result, the optimum beam waist locates at 34 km in altitude with a waist radius of 100 mm. As the long-distance propagation of laser beam in free space, the diffraction and interference effects can not be ignored. To precisely evaluate the optical performance of this specific optical system, the physical propagation model of laser should be analyzed. The Gauss beam propagation model based on the physical simulation of the above obtained LLT system is shown in Fig. 3.

As the brightness and the beam quality is highly required by the AO System, the encircled energy ratio inside a specific radius is chosen as one of the most important assessment criteria of optical performance. The amplitude of an ideal collimated Gauss beam can be represented by:

$$A(r) = a_0 exp(\frac{-r^2}{w}) \tag{6}$$

And the corresponding irradiance is calculated as:

$$I(r) = I_0 exp(\frac{-2r^2}{w}) \tag{7}$$

where $r$ denotes the light spot radius and $w$ represents the specific value of $r$ when the irradiance equals $I_0/e^2$. As expressed in Eq. (7), the beam brightness and quality is relevant to $w$, which is given by Eq. (5). Therefore, the ratio of the encircled energy of an ideal Gauss beam can be calculated as:

$$E(r=a) = \frac{\int_0^a \int_0^{2\pi} I(r) 2\pi r dr d\theta}{\int_0^\infty \int_0^{2\pi} I(r) 2\pi r dr d\theta} \tag{8}$$

The normalized irradiance distribution at 120 km is shown in Fig. 4. Only 38.09% of energy is encircled inside the circular domain with a radius of 233 mm, which cannot satisfy the science requirement as listed

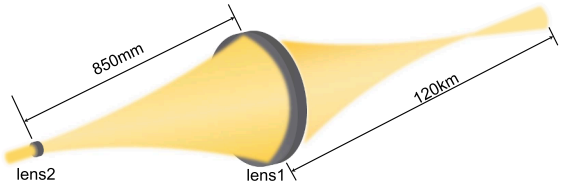


**Fig. 3.** Gauss Beam propagation of LLT.

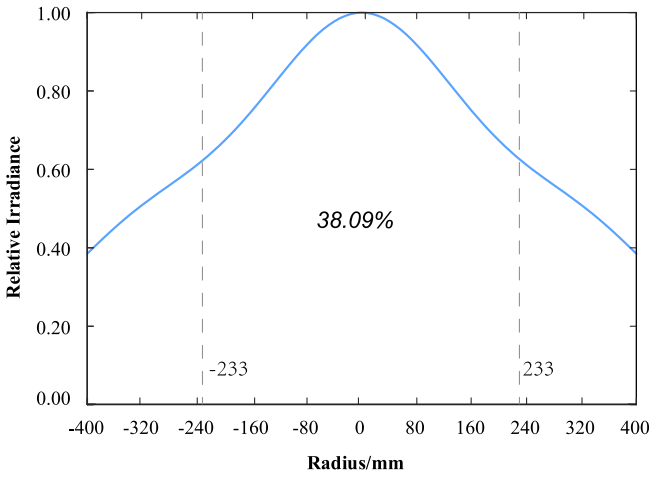


**Fig. 4.** The encircled energy ratio of the initial design.

in Table 1. This result indicates that the optical design optimization procedure under geometrical optics evaluation criterion is ineffective for the long-distance propagation of laser beam. A precise optical design is necessary, for instance, the optical design based on the physical optics theorem is needed.

### 3.3. Update the optical design using physical optics theorem

In Section 3A, the location of the beam waist is constrained in the optimization process while minimizing the RMS WFE, however, the optical performance can not meet the requirements as analyzed in Section 3B. In this Section, the merit function is replaced by the physical optics evaluation criterion. Meanwhile, the geometrical ray tracing performance should be satisfied.

As mentioned above, a shorter compensation distance is preferred considering the instrumentation, and we make a trade-off discussion of material choice to minimize the compensation distance. Three different kinds of typical optical glass including SILICA, F2, and BK7 are taken into consideration. The temperature coefficient of the absolute refractive index for a specific material can be expressed:

$$\frac{dn}{dT} = \frac{n^2-1}{2n}(D_0 + 2D_1\Delta T + 3D_2\Delta T^2 + \frac{E_0 + 2E_1\Delta T}{\lambda^2 - \lambda_{TK}^2}) \tag{9}$$

where $n$ represents refractive index relative to vacuum; $\Delta T$ is the temperature difference; $\lambda$ stands for the wavelength; $D_0$, $D_1$, $D_2$, $E_0$, $E_1$, and $\lambda_{TK}$ are constants depending on glass type. Temperature coefficient of the absolute refractive index of three different type of optical glass is shown in Fig. 5. It is obvious that F2 and BK7 has a relatively lower temperature coefficient of refractive index compared with SILICA, and we choose F2 and BK7 as the new materials for LLT and conduct the

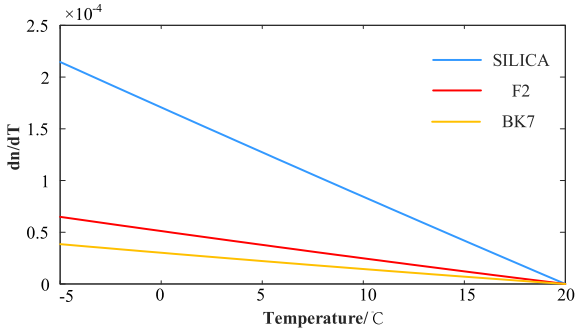


**Fig. 5.** Temperature coefficient of the absolute refractive index of three different optical glasses.

optimization with the physical optics evaluation criterion on the initial design. The distance between Lens 1 and Lens 2 is selected as a compensator. The final positions of the optical components after the optimization process are presented in Table 3. The optical performance is also evaluated by RMS WFE and the encircled energy ratio with different working temperatures. The relationship between RMS WFE and FOV is shown in Fig. 6. It shows that the optimized design shows good optical performance in terms of RMS WFE and satisfies the predefined specifications well. The largest RMS WFE is less than 0.016 l in the temperature range of −5°C to 20 °C. The compensation distance between Lens 1 and Lens 2 is reduced to 0.033 mm, which is far less than that of the initial design.

Similarly, we evaluate the encircled energy ratio within a diameter of 233 mm at 120 km in altitude, as shown in Fig. 7, wherein 96.10% energy efficiency is achieved. All of these results demonstrate the optical design based on the physical optics theorem is necessitated for the laser's long-distance propagation after the initial design is constructed based on geometrical ray tracing.

## 4. Tolerance analysis

Due to the special working environment of LLT, it is necessary to analyze its optical performance in different situations. In this research, we choose RMS WFE as the performance metric to allocate the tolerance. Assigning wavefront errors to each optical element of the LGSF system will be used to guide the fabrication of each optical component and the design of mechanical devices. The final RMS WFE budget for LLT should be limited to 0.037$\lambda$. A reasonable tolerance allocation of optical parameters is given after the sensitivity being analyzed. The estimated RMS WFE shows that the allocation can confirm to the performance deviation requirement well. As we discussed in Section 3, optical simulation based on the physical optics model is much more convinced than geometrical ray tracing. Hence, during the tolerancing process, we take the encircled energy ratio within a diameter of 233 mm at 120 km as the merit function in Monte Carlo tolerance analysis to estimate the expected physical optics propagation performance of LLT based on the allocation that we made above.

Firstly, the tolerance parameters need to be assigned. Each of the design parameters is perturbed within the range of tolerance allocation following a modified Gaussian normal distribution, which is given by:

$$p(t) = \frac{1}{\sqrt{2\pi}\sigma} exp(-\frac{t^2}{2\sigma^2}) \tag{10}$$

After the tolerance being assigned, a perturbed LLT module is created to evaluate the physical optics performance. If the enclosed energy of the perturbed module is unacceptable, a changeable parameter will be selected as a compensator. Hence, we perform the optimization of the distance between Lens 1 and Lens 2 of the perturbed module to compensate for the energy loss caused by the allocated tolerance parameter via the physical optics propagation simulation. During the optimization process, the compensation distance is restricted to 0.5 mm. If the physical optics performance of the compensated module is acceptable, the enclosed energy ratio will be output as the result of each tolerance iteration. If not, the tolerance parameters are considered tight, and the tolerance iteration will be performed again until the enclosed energy ratio is acceptable. The tolerance process is shown in Fig. 8.

This process has been implemented in each iteration to guarantee a proper compensation distance and tolerance allocation. After 400 times of Monte Carlo analysis, a reasonable tolerance allocation has been obtained as listed in Table 4 considering the achievable fabrication ability, and parts of the Monte Carlo results is shown in Fig. 9. It is obvious that the optimized system is not sensitive to fabrication when tolerance allocation is being considered. The enclosed energy ratio is

**Table 3**
Optical parameter for LLT updated design.

| Element | Material | Curvature radius(mm) | Thickness (mm) | Conic | Semi-Diameter (mm) |
|---|---|---|---|---|---|
| Lens 1-S1 | BK7 | 392.831 | 70.000 | −0.378 | 200 |
| Lens 1-S2 | | 1356.645 | 850.000 | | 200 |
| Lens 2-S1 | F2 | −82.124 | 13.000 | −0.824 | 30 |
| Lens 2-S2 | | 6546.516 | | | 30 |

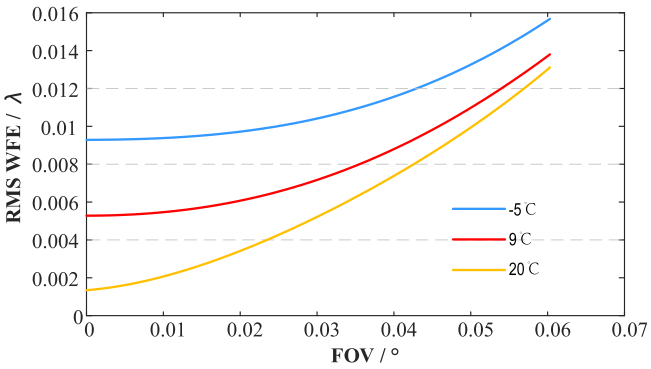


**Fig. 6.** RMS WFE vs Field of View under different temperatures.

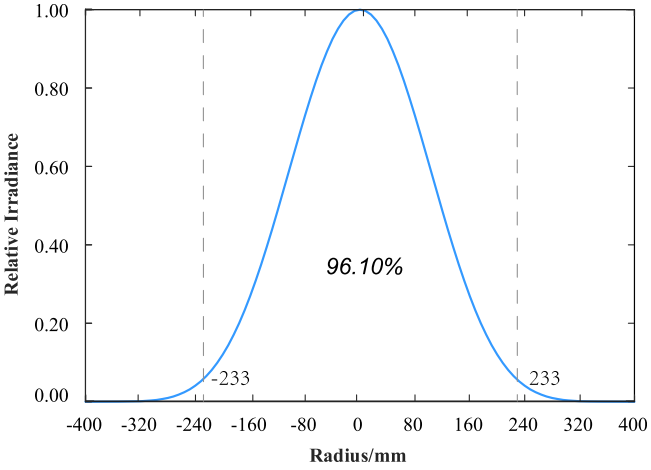


**Fig. 7.** The encircled energy ratio of the optimized design.

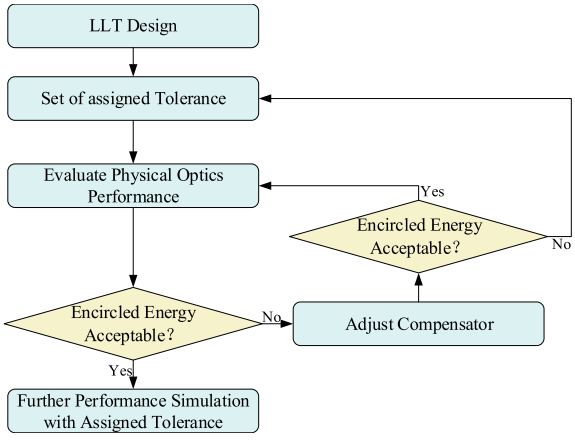


**Fig. 8.** Tolerance analysis flow chart.

**Table 4**
Tolerance allocation for LLT

| Parameters | Tolerance (mm) |
|---|---|
| Lens1 surface1 Radius | 0.1 |
| Lens1 surface2 Radius | 0.4 |
| Lens1 Thickness | 0.2 |
| Lens2 surface1 Radius | 0.1 |
| Lens2 surface2 Radius | 0.4 |
| Lens2 Thickness | 0.1 |

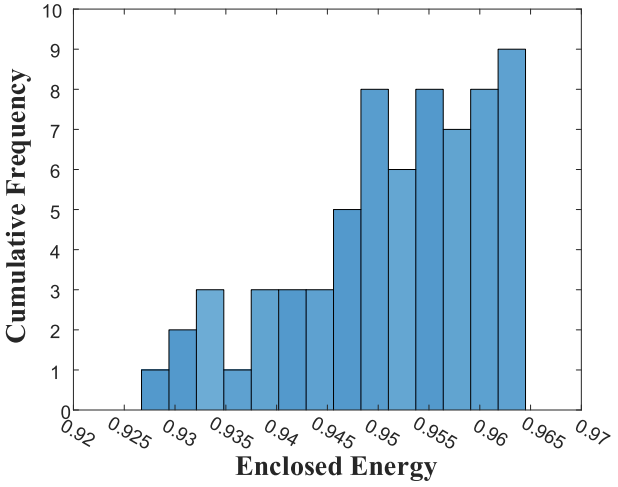


**Fig. 9.** Monte Carlo tolerance result.

larger than 92.5% for all working conditions, which demonstrates that the provided tolerance method and allocation are convinced.

## 5. Conclusion

To summarize, we have provided a recommended optical design method for laser launch telescope based on the physical optics theorem which is aimed to generate multiple laser guide stars at sodium layer. The optical design starts with the initial optical system design based on the geometrical optics assumption, and then we optimize the optical system via the physical optics theorem. Besides, the tolerance analysis is also provided to evaluate the feasibility of instrumentation based on the physics optics propagation. The simulation results show that the proposed optical design method based on precise physical optics propagation is highly rewarding and even necessitated for the laser beam propagation systems. We believe that our work might provide a good guidance for researchers to design similar laser propagation systems in the future.

## Funding

National Natural Science Foundation of China (61805088); Science, Technology, and Innovation Commission of Shenzhen Municipality (JCYJ20190809100811375, JCYJ20210324115812035); Key Research and Development Program of Hubei Province (2020BAB121); Fundamental Research Funds for the Central Universities (2019kfyXKJC040); Innovation Fund of WNLO.

## Declaration of Competing Interest

The authors declare that they have no known competing financial interests or personal relationships that could have appeared to influence the work reported in this paper.

## References

Happer, W., MacDonald, G., Max, C., Dyson, F., 1994. Atmosphericturbulence compensation by resonant optical backscattering from the sodium layer in the upper atmosphere. JOSA A 11, 263–276.
Primmerman, C.A., Murphy, D.V., Page, D.A., Zollars, B.G., Barclay, H.T., 1991. Compensation of atmospheric optical distortion using a synthetic beacon. Nature 353, 141–143.
Chin, J.C., Wizinowich, P., Campbell, R., Chock, L., Cooper, A., James, E., Lyke, J., Mastromarino, J., Martin, O., Medeiros, D., et al., 2012. Keck i laser guide star adaptive optics system. In: Adaptive Optics Systems III, vol. 8447. International Society for Optics and Photonics, p. 84474.
Chin, J.C., Wizinowich, P., Wetherell, E., Lilley, S., Cetre, S., Ragland, S., Medeiros, D., Tsubota, K., Doppmann, G., Otarola, A., et al., 2016. Keck ii laser guide star ao system and performance with the toptica/mpbc laser. In: Adaptive Optics Systems V, vol. 9909. International Society for Optics and Photonics, p. 99090S.
d'Orgeville, C., Diggs, S., Fesquet, V., Neichel, B., Rambold, W., Rigaut, F., Serio, A., Araya, C., Arriagada, G., Balladares, R., et al., 2012. Gemini south multi-conjugate adaptive optics (gems) laser guide star facility onsky performance results. In: Adaptive Optics Systems III, vol. 8447. International Society for Optics and Photonics, p. 84471Q.
Hackenberg, W., Calia, D.B., Buzzoni, B., Comin, M., Dupuy, C., Gago, F., Guidolin, I., Guzman, R., Holzloehner, R., Kern, L., et al., 2014. Assembly and test results of the aof laser guide star units at eso. In: Adaptive Optics Systems IV, vol. 9148. International Society for Optics and Photonics, p. 91483O.
Minowa, Y., Hayano, Y., Terada, H., Pyo, T.-S., Oya, S., Hattori, M., Shirahata, M., Takami, H., Guyon, O., Garrel, V., et al., 2012. Subaru laser guide adaptive optics system: performance and science operation. In: Adaptive Optics Systems III, vol. 8447. International Society for Optics and Photonics, p. 84471F.
Li, M., Jiang, C., Wei, K., et al., 2018. Design of the tmt laser guide star facility. Opto-Electron. Eng. 45, 170735.
Gross, H., Zügge, H., Peschka, M., Blechinger, F., 2015. Handbook of Optical Systems, Aberration Theory and Correction of Optical Systems, Chap 29, pp. 1–70.
Holzlohner, R., Calia, D.B., Hackenberg, W., 2008. Physical optics modeling and optimization of laser guide star propagation. In: Adaptive Optics Systems, vol. 7015. International Society for Optics and Photonics, p. 701521.
Bonaccini, D., Allaert, E., Araujo, C., Brunetto, E., Buzzoni, B., Comin, M., Cullum, M.J., Davies, R.I., Dichirico, C., Dierickx, P., et al., 2003. The vlt laser guide star facility. In: Adaptive Optical System Technologies II, vol. 4839. International Society for Optics and Photonics, pp. 381–392.
d'Orgeville, C., Bauman, B., Catone, J., Ellerbroek, B., Buchroeder, R., 2002. Gemini north and south laser guide star systems requirements and preliminary designs. In: International Symposium on Optical Science and Technology.
Boyer, C., Ellerbroek, B., Gilles, L., Wang, L., 2010. The tmt laser guide star facility. In: 1st AO4ELT Conference-Adaptive Optics for Extremely Large Telescopes, EDP Sciences, p. 04004.